



Functional Validation of Genomic and Proteomic Data

A Platform to Validate Proteins and Pathways That Alter Mitochondrial Function

Application Brief

Introduction

Comparative genomic and proteomic analyses have identified approximately half of the estimated 1,500 mitochondrial proteins encoded by the human nuclear genome. In recently published studies, Agilent Seahorse XF assays have extended these estimates through the identification of functional roles of some of the nuclear and mtDNA-encoded proteins, and in one case, clarifying assumptions about their activity that had been based on sequence homology data. For many studies, being able to establish whether mitochondria function has been altered or not is key to understanding whether bioenergetic changes are a cause or consequence of the observed phenotype.

Perocchi; *et al.*¹ leveraged data from comparative physiology, including OXPHOS studies, evolutionary genomics, organelle proteomics, and RNA interference studies to identify a product of the CBARA1 gene as the founding member of a set of proteins required for high-capacity mitochondrial calcium uptake. Named MICU1 by the investigators, this gene product is associated with the mitochondrial inner membrane, and has several characteristics required for Ca^{2+} transport, including the two canonical EF hands essential for activity.

Based on historical biochemical characterizations and the availability of RNAi reagents, the investigators used siRNA constructs targeting 13 genes expressed in reporter cell lines. One short hairpin RNA (shRNA) construct that corresponded to CBARA1 reduced mitochondrial calcium uptake and showed a strong correlation to the level of MICU1 knockdown. Complementary DNA rescue studies in MICU1 knockdown cells fully restored mitochondrial Ca^{2+} uptake.

The investigators further determined whether MICU1 knockdown affected mitochondrial membrane potential or respiration in intact cells, since Ca^{2+} uptake depends on membrane potential, and is affected by respiration. Membrane potential in MICU1-silenced cells was comparable to that of control cells, and both could be fully depolarized using the electron transport chain decoupler carbonyl cyanide *m*-chlorophenylhydrazone (CCCP). The only remaining alternative explanation for the control of Ca^{2+} uptake by MICU1 was that it was secondary to some defect of mitochondrial respiration caused by MICU1 modulation or an artifact of that modulation.



Agilent Technologies

To address this possibility, a full mitochondrial analysis was performed in MICU1-silenced or intact cells using an Agilent Seahorse XF Analyzer (Figure 1). In this analysis, several parameters of mitochondrial function were determined. The ATP-coupled respiration rate (oligomycin sensitive fraction), the maximal uncoupled rate (FCCP induced maximal rate), and the leak rate (oligomycin insensitive fraction) of respiration were similar in the two cell lines. The traces for both control and MICU1-ablated cells overlap, demonstrating that mitochondrial function was competent in both samples.

The investigators concluded that these data show that OXPHOS remains intact in MICU1-silenced cells, and that mitochondrial Ca^{2+} uptake phenotype does not occur as a secondary consequence of generalized mitochondrial dysfunction. Other studies comparing Ca^{2+} homeostasis in knockdown cells confirmed that MICU1 is required for mitochondrial uptake in HeLa cells, and that the calcium uptake phenotype in knockdown cells is independent of the Ca^{2+} agonists used.

While several mitochondrial Ca^{2+} uptake mechanisms may exist, the investigators concluded that the data described above, and other experiments, support a key role for MICU1 in regulating the calcium uniporter. Taken together, these findings show that MICU1 localizes to mitochondria, and its loss impairs mitochondrial Ca^{2+} uptake in a manner that depends on its EF hands, without impairment of mitochondrial function.

Results and Discussion

Several additional studies demonstrate the utility of combining genomic, proteomic, and functional analysis for protein characterization. Miczuk; *et al.*² clarified the role of c17orf42, or transcription elongation factor of mitochondria (TEFM) in mitochondrial transcription. The authors identified this gene as a putative human mitochondrial Holliday Junction Resolvase (HJR) based on its sequence homology with the bacterial gene. However, they found that this hypothesis was not supported

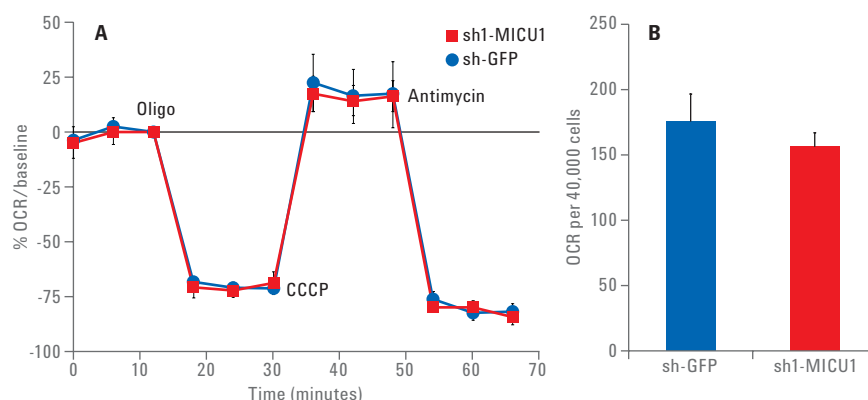


Figure 1. Mitochondrial respiration remains intact in MICU1-silenced cells. A) Normalized OCR in sh1-MICU1 and sh-GFP after addition of the complex V inhibitor oligomycin (Oligo, 0.5 μM), uncoupler CCCP (0.5 μM), and complex III inhibitor antimycin (0.5 μM). The ATP-coupled respiratory rate, the maximal uncoupled rate, and the leak rate were similar in control and sh1-MICU1 knockdown cells, indicating that the mitochondrial Ca^{2+} uptake phenotype of MICU1-silenced cells is not a consequence of generalized mitochondrial dysfunction. B) Basal oxygen consumption rate (OCR, $\text{pmol O}_2/\text{min}$) in control and knockdown cells. Error bars indicate mean \pm s.d.

experimentally, as recombinant TEFM isolated from human mitochondria, or purified from *E. coli* lacked resolvase activity.

To test the role of TEFM in OXPHOS function, TEFM expression was inactivated by RNA interference in HOS cells. TEFM RNAi knockdown markedly reduced complex IV subunit, COX2 and NDUF8, a complex 1 component. A 50 % reduction in OCR as determined by Agilent Seahorse XF analysis, and an uncoupling of the respiratory control ratio accompanied the decrease in respiratory chain components. The authors concluded that TEFM plays a key role in mitochondrial energy production, and that given its homology to nucleic acid modifying proteins, this role likely occurs through its contribution of mtDNA maintenance or expression.

Telomere dysfunction, associated with many aspects of aging, activates p53-mediated arrest of cellular growth, senescence, and apoptosis. To determine whether telomere shortening and dysfunction could also be linked to diminished mitochondrial biology, oxidative defenses, and metabolism, Sahin; *et al.*³ used mouse models successively bred for telomerase deficiency and dysfunction. These animals exhibit progressive telomere

shortening, with increasing atrophy and functional decline across proliferative organs (intestinal, hematopoietic) and quiescent organs (liver and heart) that do not exhibit significant apoptosis.

Transcriptome profiling from both tissue types showed strong enrichment for networks regulated by PGC-1 α and PGC-1 β including OXPHOS, mitochondrial function, oxidative stress, and gluconeogenesis, with the most prominent network perturbations in repressed OXPHOS genes, which are characterized by many PGC targets.

Telomere dysfunction correlated with marked declines in mitochondrial function, as determined by XF analysis, of isolated heart and liver mitochondria. This finding was substantiated by showing that PGC overexpression *in vivo*, could reverse the mitochondrial defect as measured by the Agilent Seahorse XF Analyzer in isolated liver mitochondria after adenoviral PGC delivery. The authors concluded that combined transcriptomic, molecular, genetic, and functional analyses on cellular and organismic levels established a molecular link between telomere dysfunction and repression of PGC-dependent processes of mitochondrial biogenesis, function, gluconeogenesis, and oxidative defense.

Materials and Methods

Cells and compounds

HeLa cells were grown in DMEM high-glucose medium with 10 % FBS at 37 °C and 5 % CO₂. The cells were seeded in Agilent Seahorse XF24 Cell Culture Microplates at 40,000/well for ~20 hours. One hour prior to the assay, the growth medium was removed from each well and replaced with unbuffered DMEM (Dulbecco's modified Eagle's medium, pH 7.4) supplemented with 4 mM L-glutamine (Gibco).

Oligomycin, CCCP, and antimycin A were from Sigma (Now available as a kit from Agilent).

XF Bioenergetic analysis

XF analyses were performed in an Agilent Seahorse XF Analyzer a fully integrated, multi-well instrument that measures the uptake and excretion of metabolic end products in real time. Oxygen consumption rates (OCRs) and extracellular acidification rates (ECARs) were measured using Agilent Seahorse XF FluxPaks. The disposable assay kits include a solid state sensor cartridge embedded with dual fluorescent biosensors (O₂ and H⁺). Each sensor cartridge is also equipped with four drug delivery ports per well for injecting agents during an assay.

OCR and ECAR measurements were carried out as previously described⁴, and as illustrated in Figure 2. After the HeLa cells were switched from culture medium to assay medium, the sensor cartridge was loaded with experimental compounds, calibrated, and placed over the culture plate containing the prepared HeLa cells.

The preloaded oligomycin, CCCP, and antimycin A were injected sequentially to final concentrations of 0.5 μM for each compound. This determined the basal oxygen consumption, the oxygen consumption linked to ATP production, the level of non-ATP-linked oxygen consumption (proton leak), the maximal respiration capacity, and the non-mitochondrial oxygen consumption.

Conclusion

These studies demonstrate the power of integrating genomics, proteomic, and functional analyses, including cellular bioenergetic analysis, using XF analysis, for assigning functional roles to proteins.

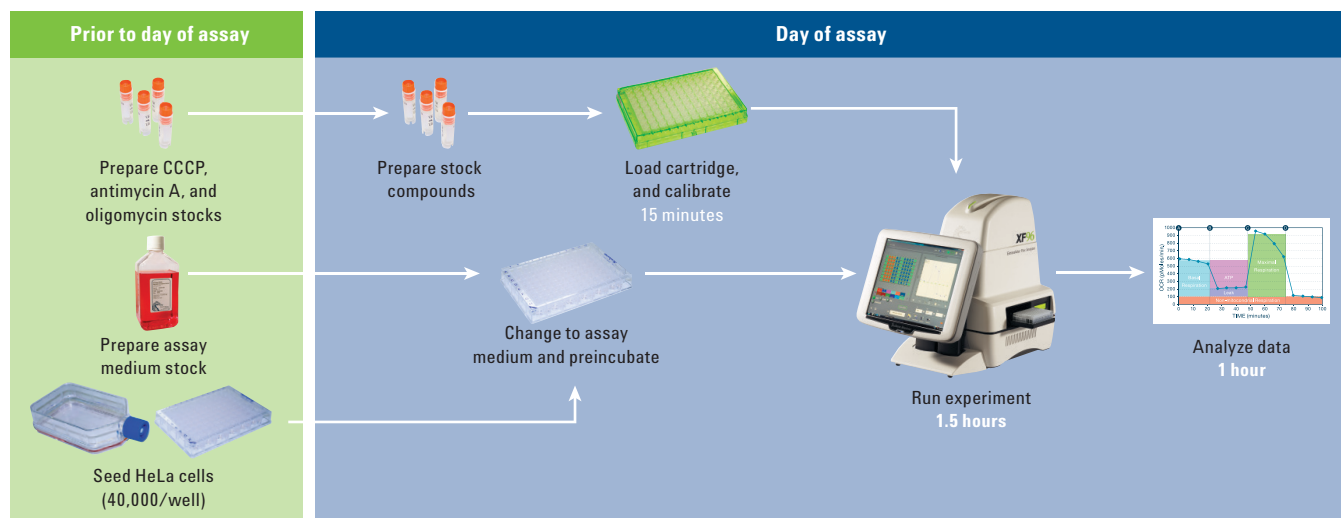


Figure 2. Flow chart of the XF assay.

References

1. Perocchi, F.; *et al.* MICU 1 encodes a mitochondrial EF hand protein required for CA(2+) uptake. *Nature* **2010**, *467*, 291-96. Epub 2010 Aug 8.
2. Minczuk, M.; *et al.* TEFM (C17orf42) is necessary for transcription of human mt.DNA. *Nucleic Acids Res.*, *201*, 1-16. PMID 21278163.
3. Sahin, E. W.; *et al.* Telomere dysfunction induces a metabolic and mitochondrial compromise. *Nature* **2011**, *470*, 359-65.
4. Gohil, V. M.; *et al.* Nutrient sensitized screening for drugs that shift energy metabolism from mitochondrial respiration to glycolysis. *Nature Biotechnol.* **2010**, *28*, 249-255.

www.agilent.com

For Research Use Only. Not for use in diagnostic procedures.

This information is subject to change without notice.

© Agilent Technologies, Inc., 2016
Published in the USA, December 1, 2016
5991-7131EN



Agilent Technologies